Morphotectonic analysis of the long-term surface expression of the 2009 L'Aquila earthquake fault (Central Italy) using airborne LiDAR data

Keywords: active normal faulting; tectonic geomorphology; airborne LiDAR; 2009 L'Aquila earthquake

Authors: Riccardo Civico[1*], Stefano Pucci[1], Paolo Marco De Martini[1] and Daniela Pantosti[1]

[1] Istituto Nazionale di Geofisica e Vulcanologia, Rome, Italy
*Corresponding author

Abstract

In this paper we present a morphotectonic study of the Paganica-San Demetrio fault system (PSDFS) responsible for the Mw6.1 April 6, 2009 earthquake (L'Aquila, central Italy).

The discrepancy observed between the length of the seismologic-geodetic modeled fault, the limited size of the primary coseismic surface ruptures and the significant morphological expression of the PSDFS stimulated a debate about the maximum rupture length of the PSDFS and its capability to generate larger magnitude events.

To image the PSDFS long-term morphological expression and define its surface geometrical arrangement (length, number of fault splays and boundaries), we took advantage of a high-resolution airborne LiDAR dataset. LiDAR topography substantially increased our confidence in detecting even subtle tectonic-controlled morphologies. We define the PSDFS as a ~19km-long fault system that displays a complex structural setting characterized by two different sectors: 1) the Paganica sector to the NW, with a narrow deformation zone, and 2) the San Demetrio sector to SE, where the strain is accommodated by several fault-splays dissecting a wider Quaternary basin. We also defined a first-order hierarchy among the numerous fault splays across the PSDFS.

The long-term geomorphic expression of the PSDFS suggests that it ruptured also involving the whole 19km-long structure besides rupturing only small sections, as it occurred in 2009. This suggests a variable slip behavior.

Empirical relations applied to this hypothesis allow up to M 6.6 earthquakes along the PSDFS. These results have a critical impact on the seismic hazard assessment of the area when compared with a M 6.1 event as the 2009.

1 Introduction

On April 6, 2009, a Mw 6.1 earthquake (Herrmann et al., 2011) struck a densely populated region in the Abruzzi Apennines and was felt in a wide area of central Italy (figure 1). Due to its location and

relatively shallow hypocentral depth (~10 km), the earthquake caused heavy damage in the town of L'Aquila and surrounding villages and resulted in more than 300 fatalities and thousands of injured.

Seismological and geodetic data converge in identifying, as the 2009 earthquake causative fault, a NW-striking, SW-dipping, normal fault, but with different lengths varying between 12 and 18.5 km (figure 1 and figure 2). The location of this fault coincides with a complex fault system bounding to the east the Middle Aterno Valley (hereinafter referred to as 2009-earthquake fault system). Primary, continuous coseismic surface ruptures (0.15 m of throw and ~0.1 m of opening) were observed for about 3 km (Emergeo Working Group, 2010; Vittori et al., 2011) along the northern portion of this system (Paganica fault - figure 2), and occurred along pre-existing composite fault scarps, affecting mainly Quaternary deposits, with throws of tens of meters and lengths of several km (Pucci et al., 2014). Sparse and faint ground ruptures were observed to extend both to the NW and to the SE (figure 2; see also Vannoli et al., 2102).

The long-term morphological expression of this fault system (i.e. the Quaternary basin developed on its hangingwall) does not fit (both in terms of size and length) with the limited size and extent of the 2009 primary coseismic surface ruptures. Cinti et al. (2011) on the basis of paleoseismic investigations, hypothesize provide evidence that the prominent scarps characterizing the fault system result from longer and larger earthquake ruptures with respect to the 2009 event, thus opening the possibility for larger magnitude events.

Because of the relevance of this hypothesis for the seismic hazard of the area, we undertook a detailed morphotectonic study of the 2009-earthquake fault system in order to define its maximum length and earthquake potential.

To reach this goal we took advantage of high-resolution airborne LiDAR data that, integrated with the interpretation of aerial photographs and supported by extensive field-truthing (including the data presented in Pucci et al., 2014), allowed us to understand the geometry, extent, arrangement at the surface, permanent boundaries and internal complexity of the 2009-earthquake fault system.

This approach based on LiDAR-derived high-resolution topography is the first application in Italy for active tectonic studies and is well suited to be reproduced for other active faults in the region, that is one of the most seismic of Italy.

In the following chapters we present a brief seismotectonic setting of the earthquake area, the applied methodology, the mapping of the fault system and the scarp throw estimates. Finally, we discuss the results from the morphotectonic analysis with respect to fault segmentation and seismic potential of the 2009 earthquake causative fault.

2 The seismotectonic context of the Mw 6.1 April 6, 2009 L'Aquila earthquake

The Mw 6.1 April 6, 2009 L'Aquila earthquake and sequence (Herrmann et al., 2011) occurred in the central Apennines. This mountain chain is part of a northeast-verging imbricate thrust-and-fold mountain belt that, since late Pliocene, has been dissected by intense extensional tectonics resulting

from the eastward migration of the Apenninic compressional front (Malinverno and Ryan, 1986; Cavinato and De Celles, 1999). The Apennines extensional belt comprises active and seismogenic normal and normal-oblique faults, mainly NW-SE and NNW-SSE striking. These are arranged in systems paralleling the physiographic and structural axis of the chain and, generally, not exceeding 30 km in length. These faults offset or locally reactivate structures belonging to the compressional phase.

These normal fault systems have controlled the development of several intermontane tectonic depressions partially filled with sequences of Plio-Quaternary continental deposits, up to hundreds of meters-thick (Cavinato & De Celles, 1999).

Beside the 2009-earthquake fault system, several normal faults occur in the area hit by the 2009 earthquake (Pettino and Stabiata faults in the northern Aterno River valley, Middle Aterno Fault System and Barisciano-S.Pio Fault, hereinafter referred to as UAFS, MAFS and BSPF, respectively). These are well-known in the available literature (figure 1 and figure 2 – Galli et al., 2008 and references therein). These faults have average strikes ranging from 110° N to 140° N, dip to the SW, are 9 to 15 km-long and appear to be individual structures, isolated from the 2009-earthquake fault system by the presence of geometrical/structural discontinuities.

The current rate of extension is generally perpendicular to the Apennines axis (Montone et al., 2012 and references therein), and is estimated in 2–3 mm/year from GPS (Hunstad et al., 2003; D'Agostino et al., 2011). Extension is confirmed also by focal mechanisms of earthquakes of the last decades. The historical record (http://emidius.mi.ingv.it/CPTI) reports that the Abruzzi region has been repeatedly hit by large magnitude, destructive earthquakes: the 1349, 1703, and 1915 events (all having M≥6.5 and I>10 MCS) that occurred within ~35 km from the 2009 epicenter and several smaller but closer ones that are the 1461 Maw 6.4, the 1762 Maw 5.9 and the 1791 Maw 5.4 earthquakes (Maw = average weighted Magnitude derived from macroseismic intensities [http://emidius.mi.ingv.it/CPTI04]).

The analysis of the instrumental seismicity in the area shows low levels of seismicity during the past 20 years with epicentral depths of max 12-15 km, typical of the central Apennines (Chiarabba et al., 2005). The 2009 L'Aquila earthquake sequence fully fits in this seismotectonic context: seismologic, geodetic, InSar, and geological data all depicts the Mw 6.1 April 6, 2009 mainshock causative fault as a NW-SE oriented, SW-dipping structure (Vannoli et al., 2012; Chiaraluce, 2012 and references therein), located to the east of the Middle Aterno valley (figure 1 and figure 2). Notwithstanding the high quality of available data, the moderate size of the mainshock involves a great variability in the modeling and interpretation of the length of the causative fault at depth, which ranges from 12 to nearly 19 km.

The earthquake produced an extensive and complex set of surface coseismic deformations, involving an area of hundreds of km^2 and arranged in a pattern typical for a M~6 earthquake, (Dramis & Blumetti, 2005). Continuous surface faulting (~3km-long with maximum throw of 0.15m) occurred near the Paganica village, along the base of a prominent cumulative fault scarp (up to 20 m-high) part of the Paganica Fault (hereinafter PF - figure 2, yellow triangles). Both to the north and to the south of this

section, the surface ruptures fade out and discontinuous open fissures occurred along similar trends (figure 2, green triangles).

Although there is a general agreement on the recognition of the ~3km-long primary coseismic ruptures, depending on whether or not all the discontinuous ruptures are interpreted as evidence of coseismic slip on the causative fault at depth, the estimated surface faulting total length ranges between 3 and 19 km (Falcucci et al., 2009; Boncio et al., 2010; Emergeo Working Group, 2010; Galli et al., 2010; Vittori et al., 2011; Gori et al., 2012).

The 2009-earthquake fault system was reported in some of the pre-2009 L'Aquila earthquake maps along with other fault system (Galli et al., 2008 and references therein); however, its several splays were only roughly depicted (as for the case of the PF and the San Demetrio fault, hereinafter SDF – figure 2) or missing and, as a whole, it was poorly characterized (Bagnaia et al., 1992; Vezzani and Ghisetti, 1998; Boncio et al., 2004; Geological Map of Italy - Servizio Geologico d'Italia, 2006).

There is still an open debate on the maximum extent of the coseismic rupture that may occur on the eastern flank of the Middle Aterno valley and on its capability to occur on the whole or part of this fault system, or even to extend to other "external" fault systems. This has a direct relevance for the prediction of expected magnitude of future earthquakes and, consequently, for seismic hazard assessment. In fact, Galli et al. (2010, 2011) envisage the linkage of PF and SDF with the Upper Aterno Valley Fault System to the NW (UAFS – Galadini & Galli, 2000), during the Maw 6.7 February 2, 1703 seismic event (figure 1). Differently, Moro et al. (2013), hypothesize a similar scenario but without the linkage of the SDF.

The occurrence of the 2009 L'Aquila event triggered a significant number of studies aimed at better defining the structural setting, the long-term morphological expression at surface and the paleoseismic history of the fault system responsible for the earthquake (Galli et al., 2010; 2011; Cinti et al., 2011; Civico, 2012; Giaccio et al., 2012; Gori et al., 2012; Improta et al., 2012; Blumetti et al., 2013; Moro et al., 2013; Pucci et al., 2014; Villani et al., 2014). Based both on the surface (Galli et al, 2010; Civico, 2012; Giaccio et al., 2012; Pucci et al., 2014) or on the subsurface data (Improta et al., 2012), all these studies highlighted that this fault system comprises multiple sub-parallel active splays forming a complex structure with an overall length of 12 to 19 km and an up to 250 m deep depocenter in its hangingwall. However, the relationships of the PF with nearby faults and particularly with the SDF are still matter of debate (Galli et al, 2010; Civico, 2012; Giaccio et al., 2012; Gori et al., 2012). The independence or connection of the PF with SDF has a critical relevance for estimating the Mmax (ranging between Mw 6.1 and Mw 6.7) of the earthquake they can generate, having a substantial impact on the local seismic hazard.

Cinti et al. (2011), Galli et al., (2010; 2011) and Moro et al., (2013), performed paleoseismological investigations at different sites across the PF in order to reconstruct its Late Pleistocene - Holocene rupture history. By interpreting the paleoearthquake record together with the PF long-term expression, Cinti et al. (2011) conclude that there are indications for earthquakes in the past more energetic than the April 6, 2009, likely related to the linkage between the PF and the SDF.

3 Methodology

By using airborne LiDAR and field survey, we started a detailed morphotectonic analysis of landforms and deposits affected by cumulative offsets that can be related to repeated coseismic displacements along the fault traces of the 2009-earthquake fault system. The detailed investigation area extends between Collebrincioni to the NW, Ripa to the SE, the bedrock footwall of the 2009-earthquake fault system to the east and the flat valley to the west (figure 2).

Collebrincioni and Ripa represent the natural structural boundaries that isolate the 2009-earthquake fault system from the adjacent fault systems. More in detail, based on the tectonic and geomorphic expression, the northern boundary of the 2009-earthquake fault system is interpreted to be near the Collebrincioni village. Here, a series of WNW trending, right, en echelon splays, with a deviation of ~20° with respect to the average strike of the 2009-earthquake fault system occur and may act as a structural boundary. The southern boundary of the system coincides with the southern edge of the Middle Aterno basin and with a deviation (~20° to the east) of the tectonic structures trend with respect to the average strike of the 2009-earthquake fault system, as shown by fault splays to the south of Ripa (figure 2).

The investigated area appears to be strongly controlled by tectonics that dissected the landscape producing a staircase-like arrangement of flat, remnant land surfaces separated by scarps (more abundant in the southern portion).

Several patches of these remnant surfaces were identified and mapped. These include both erosional surfaces carved on the local bedrock and/or depositional surfaces of alluvial Quaternary deposits, that represent the local base level of an ancient drainage network (figure 3); most of these surfaces are located in the southeastern portion of the basin and lie at different elevations with respect to the present-day basin floor (for details see also Pucci et al., 2014). The extensive morphotectonic analysis was integrated by new, fundamental geological field data (Pucci et al., 2014) aimed at defining the extent of outcropping Quaternary deposits (figure 4).

The geological data evidenced an extensive cover of lacustrine and fluvial/alluvial Quaternary deposits, generally separated by unconformities, accumulated on top of a mainly Cretaceous-Miocene carbonate bedrock. The continental deposits overlying the bedrock sequence can be referred to two main cycles: 1) a lower (Early-Middle Pleistocene) fluvio-lacustrine cycle, >200 m thick, including whitish carbonate lacustrine silts (S. Nicandro Fm.), etheropic with deltaic and alluvial fan deposits (Vall'Orsa and Valle dell'Inferno Fms.) including conglomerates and slope-derived carbonatic breccias (Valle Valiano and Fonte Vedice Fms.); 2) an upper fluvio-alluvial cycle (Middle Pleistocene), carved in the former one and consisting of silts and sands rich in volcanic ashes and rounded carbonate gravels (S. Mauro Fm.). All these deposits are covered by Late Pleistocene-Holocene fluvial/alluvial sediments, mainly related to the Aterno River, and by slope debris and colluvial deposits (Pucci et al., 2014).

Among all the linear and planar morphological features that can contribute to the identification of possible tectonic lineaments (scarps, base of scarps, displaced alluvial fans, abrupt slope angle changes,

paleosurfaces, hinge line of saddles and ridges, inner and outer edge of paleosurfaces, terrace risers, wind gaps, paleovalleys, degree of incisions, drainage diversions, etc.), we devoted particular attention to the study of tectonic scarps. In fact, the latter are known to be particularly effective for the estimate of geometrical and behavioral parameters of active faults and for the reconstruction of the characteristics of the earthquakes (slip models) that concurred to their growth (Wallace, 1977; King et al., 1998; Stein et al., 1998; Cowie & Scholz, 1992; Nicol et al., 1997; Mouslopoulou et al., 2009).

In slow deforming tectonic environments such as Italy, Greece or Spain (Perea et al., 2006; Galli et al., 2008; Caputo et al., 2012), fault-related scarps are generally small and strongly affected by degradational and aggradational processes that modify their original shape. As a consequence, fault-related scarps are difficult to identify and to map with small uncertainties by means of conventional tools such as aerial photographs, satellite imagery, or low-resolution digital elevation data. Moreover, in some cases the identification of such morphological features is made difficult because of the presence of highly vegetated and urbanized areas.

Excluding any man-made feature, these morphological features can be produced by both tectonic and erosive/depositional processes. For our purpose, a tectonic origin was assumed when at least one of these conditions is established: a) the linear feature is independent and far from the influence of the of erosive/depositional processes (e.g. fluvial or lacustrine dynamics); b) the lineament is represented by a scarp that trends parallel or sub-parallel to other known fault traces; c) the lineament is a lateral continuation of a clearly identifiable fault-trace (see also Begg and Mouslopoulou, 2010).

For the reasons above, to investigate the 2009 earthquake fault system, we integrated high-resolution airborne LiDAR (Light Detection And Ranging, also known as Airborne Laser Swath Mapping or ALSM) data with interpretation of 1:33,000 scale aerial photographs (Gruppo Aereo Italiano – GAI, 1954/1955), other raster imagery (Digital Elevation Model - DEM 5m; Istituto Geografico Militare – IGM 1:25.000 topographic maps; Orthophoto Abruzzo 2007) and extensive field survey.

Airborne LiDAR is a recent technology that allows rapid and high-resolution measurement of topography over large areas. Because the resolution can be well smaller than 1m, LiDAR-derived topographic data have the potential to substantially increase the confidence to reveal active fault traces through an enhanced visualization and consequent identification and mapping of fault scarps and other morphological features related to tectonic activity. The airborne LiDAR survey of the study area was performed a few days after the 6 April 2009 mainshock by the Civil Protection of Friuli Venezia Giulia (Italy) using an Optech ALTM 3100 EA Airborne Laser Terrain Mapper System. The original LiDAR bare-earth point cloud was processed in order to obtain a regular 1 x 1 m Digital Elevation Model (DEM) and several derivative digital maps (shaded relief, slope, aspect, etc.). More details are provided in the supplementary materials section.

4 Fault system geometry

The 2009-earthquake fault system comprises several sub-parallel splays, characterized by a predominant dip-slip kinematics (figure 4).

At a basin-wide scale, we imaged a complex structural setting at the surface, characterized by the presence of more than 15, aligned and/or parallel normal fault splays, frequently arranged in a quasi-fractal sequence of horst and graben of variable size. Fault splays are defined as a set of fault traces, including both synthetic and antithetic elements, that are aligned (with a deviation up to 10°) or stepped/overlapped (tens of meters). Individual fault splays display an average strike of 140° N and an average length of 4500 m.

As a rule, we named all the fault splays using the prefixes P and S to differentiate between those close to Paganica or to San Demetrio Ne' Vestini villages, respectively, and numbered them starting from the basin toward the footwall (e.g. P1 stands for splay number 1 in the Paganica sector, S6 for splay number 6 in the San Ne' Vestini sector – figure 4).

Looking at the surface pattern, we can distinguish two main sectors characterized by different structural arrangements and by a different extent of the Plio-Pleistocene and Holocene deposits (figure 4). In the Paganica sector (northern portion), the basin is characterized by a limited extent of outcropping Quaternary deposits and the deformation is accommodated by a narrow fault zone comprising 5 main 400-500 m-spaced fault splays, forming a less than 2 km-wide deformational band. In the San Demetrio Ne' Vestini sector (southern portion), the structural arrangement becomes more complex and the deformation appears to be accommodated by several tectonic structures, creating a wider fault system with respect to the northern area. In fact, here the fault system forms a staircase landscape (up to 11 parallel, ~1km-spaced fault traces) and exhumes and dissects a larger Quaternary basin.

5 Along-strike distribution of the morphological throws

To better understand the significance of the 2009 causative fault system within the adjacent active fault systems described in the literature (UAFS, MAFS and BSPF, figure 1 and figure 5), we focused on the comparison of their cumulative vertical displacements as recorded in the landscape, assuming a purely tectonic origin. We constructed 36 topographic profiles between the basin floor and the highest footwall surfaces (remnants of an old, uplifted erosional landscape – Galadini et al., 2003; Blumetti et al., 2013) drawn, in most of the cases, on the high-resolution LiDAR-derived DEM. To do so, we tried to intersect the best-displaced geomorphic marker and, as a consequence, profiles are not equally spaced and have lengths ranging between 5200 m and 11000 m (figure 5).

Total vertical displacement (i.e. minimum net throw) across each fault system has been measured as the difference between the maximum elevation of their footwall (remnant top surfaces in figure 5 a- b and 6a) and the minimum elevation of the basin floor at the hangingwall (figure 6a), while morphological throws for each individual fault splay has been measured as the vertical component of the separation (Vs) between an upper and a lower reference surface values (figure 6b). Morphological throws range from 5 m to 615 m.

We investigated the along-strike throw distribution across the fault systems by plotting on a reference baseline (orange thick solid line in figure 5) the morphological throws measured from the 36 topographic profiles. The resulting plot is shown in figure 7.

In this figure, the gray area represents the total morphological throw, with maxima depicting a slightly decreasing trend toward the SE (dashed line - maximum displacements variable between ~950 and ~650 m). Two sharp drops of throw values occur close to the areas of persistent displacement deficit. This reflects on the position of major drainage incisions, as is the case for Raiale and Valle Valiano catchments (figure 5). Looking at the relative contributions of individual fault systems (colored patterns in figure 7), we note that the throw values related to each of them tend to zero near the tips of the 2009 causative fault, as imaged from the coseismic data. Moreover, the long-term throw distribution in coincidence with the 2009 causative fault, which is related to the activity of the fault system bounding the Middle Aterno Valley, approximates a symmetric bell-shaped curve with maximum throw-values at the center. The tips of this morphogenic fault system are placed southeast of the village of Collebrincioni (to the NW), in coincidence with a series of WNW trending en-echelon fault splays and near Ripa village (to the SE) (Figure 4).

This displacement pattern, although produced by a complex fault arrangement at the surface, is well comparable to that of a ~19 km-long isolated individual extensional fault (Dawers et al, 1993; Cartwright et al., 1995; Contreras et al., 2000; Nicol et al., 2005; Manzocchi et al., 2006), likely imaging the 2009 fault at depth.

The fault system bounding the eastern flank of the Middle Aterno Valley was already described by Bagnaia et al. (1992), as ~15 km-long isolated normal fault system between Paganica and San Demetrio and named Paganica – San Demetrio Fault System (hereinafter PSDFS). Given the consistency of our observations with the conclusions of Bagnaia et al. (1992), we decided to use the same nomenclature.

We also measured the morphological throws for each individual fault splay of the PSDFS, that are highlighted in figure 8 with different colors and different symbols, to distinguish between vertical throw values calculated from offset reference surfaces (i.e. piercing points) carved in bedrock or in unconsolidated deposits or a combination of the two. Basin-bounding fault splays P4 and S10 appears as the most relevant in the whole system (figure 8), displaying maximum vertical displacements of 615 m and 370 m, respectively.

Figure 9 contains the same data of figure 8 but with aggregation of the contribution of selected fault splays of the PSDFS. The black solid line is the morphological throw, the red solid curve represents the aggregation of all the individual fault splays, whereas the violet and pink areas are the P4 and S10 throw contributions, respectively. The green and blue areas highlight the aggregated contribution of the splays affecting Quaternary deposits, for the Paganica and San Demetrio sector, respectively.

A first-order consideration is that two different behaviors emerge from the plot of figure 9: from profile 0 to profile 14 the sum of the contributions of all individual fault strands (red curve) mimics both shape

and magnitude (81%) of the total deformation (black line). Conversely, from profile 15 to 29, this sum accounts for only the 61% of the morphological throw.

Also the amount of deformation related to the other intra-basin tectonic structures affecting the Quaternary deposits (green and blue areas in figure 9) appears to be different between the two sectors. The Quaternary intra-basin fault splays in the Paganica area account for an average ~15% of the total deformation, with a maximum value of ~25%, while in the San Demetrio sector the amount of deformation reaches values of ~40% (average) and ~70% (maximum). It is interesting to note that the relative contribution of the intra-basin Quaternary tectonic structures tends to become predominant in the San Demetrio sector, in coincidence with the decrease in throw values measured for splay S10 (Figure 9). These observations show that the distinction between the two sectors is not only geometrical.

6 Discussion

6.1 Tectonic style of the PSDFS

The preliminary reconstruction of the PSDFS morphology and structural arrangement suggests the persistence of the deformation from pre-Quaternary times and for its whole length. In fact, the cumulative displacement distribution along strike of the PSDFS approximates a symmetric bell-shaped curve (figure 7), reproducing a throw profile comparable to that typical of a single individual extensional fault. However, the different number and spacing of the identified fault splays, as well as the different extent of the Plio-Pleistocene and Holocene deposits that characterize the Paganica (to the NW) and San Demetrio (to the SE) sectors (figure 4), highlight that the deformation across the PSDFS is distributed in a narrow and rather simple zone to the NW and in a wide and complex zone to the SE.

Within this frame, different splays may have being active over different time intervals. For example, the relative contribution of the fault splays affecting Quaternary deposits (green and blue areas in figure 9) to the total strain of the PSDFS is substantially smaller for the Paganica sector with respect to the San Demetrio sector. This could be explained, on the one hand, by the persistence of the deformation across a narrow zone in the Paganica sector, which reflects in a stable position of the basin depocenter with the development of a relatively narrow Quaternary basin. On the other hand, the complex structural arrangement and width of the fault system in the San Demetrio sector, together with the presence of Quaternary deposits progressively younger and less elevated toward the present Aterno River bed, indicate a progressive migration in time of the basin depocenter (and thus migration of fault activity) toward the present-day valley bottom (Civico, 2012; Pucci et al., 2014).

These two different settings appear also from the morphological throw plot of figure 9. Excluding the possibility that the larger difference between the morphological throw (black solid line) and the sum of all tectonic contributions (red solid curve) is due to a systematic bias introduced by the morphological throw measurements only in the San Demetrio sector, a possible interpretation is that this can be

evidence of syntectonic deposition occurring mainly in the San Demetrio sector, where a much greater amount of Quaternary deposits are found. This syntectonic component cannot be measured at the surface and thus could result in a possible underestimation of the morphological throw values.
However, we cannot rule out the possibility that the abovementioned difference could be related to the presence of an inherited paleotopography of the area, likely associated with a previous different deformational phase.

6.2 Fault splay hierarchy

The preservation, continuity, as well as the morphological throws of the identified fault splays concurred to define also a first-order hierarchy among all the tectonic structures that characterize the morphological expression of the PSDFS at surface, depending on the different contribution of individual fault splays to the overall deformation across the fault system.
Looking at figure 8, we note that most of the deformation of the PSDFS is accommodated by two fault splays: P4 and S10. These affect mainly the bedrock and are the easternmost splays bounding the basin. This is quite expected for a normal fault, as these should be the oldest and with the longest record of deformation. Conversely, among the fault splays affecting mainly the Quaternary deposits (last ~2Ma), the most important contribution to the overall surface deformation is given by fault splays P3, S6 and partially P2. These fault splays complement each other geometrically and kinematically to produce a coherent structure (figure 10) and have a prominent geomorphic expression. The lack of clear surface evidence of fault-related deformation between these splays in the central portion of the PSDFS (NW of Poggio Picenze village – figure 10) can be related to the presence of a Late Pleistocene (ca. 27 ka - Civico, 2012) alluvial fan likely burying/eroding the fault-related cumulative morphology. These fault splays, if linked, represent the most active surface trace of the PSFDS during the Quaternary. This hypothesis is also supported by the fact that the ~3 km-long continuous 2009 coseismic rupture occurred mostly along fault splay P3 (figure 10).
High-resolution shallow seismic profiling (Improta et al., 2012, see section 3) in the Paganica sector showed the presence of two buried SW-dipping fault splays (P0 and P1 in the map of figure 4) that involve bedrock and basin infill deposits with throw values of ~100 m and ~150 m. The surface projection of fault splay P0 coincides with the occurrence of some aligned but highly discontinuous 2009 coseismic surface ruptures (figure 10). These splays do not show a clear morphological expression because of their location in the active hangingwall of the fault system and of the local high depositional rates related to the Raiale River sediment discharge (figure 2 and figure 5).
In this light, the along-strike linkage would not be limited to P3, P2 and S6 but appears to involve all the splays located at their hangingwall. In fact, fault splay P3 to P0 and S6 to S1 show a comparable arrangement suggestive of a strong simplification of the PSDFS during the Quaternary (fault maturity?).

6.3 PSDFS length

On the basis of the PSDFS long-term expression and of its relation with adjacent fault systems as mapped in previous compilations, we define its actual extent and permanent boundaries.

We found out that most of the deformation on the eastern flank of the Middle Aterno Valley appears to be accommodated by the PSDFS, whose throw profile actually approximates a symmetric bell-shaped curve with maximum throw-values at the center, reproducing a displacement pattern comparable to that of an isolated individual extensional fault (Dawers et al, 1993; Cartwright et al., 1995; Contreras et al., 2000; Nicol et al., 2005; Manzocchi et al., 2006 - figure 7). On this basis, the tips of the bell-shaped curve represent the fault boundaries that can be considered stationary at least for the last morphogenic phase of landform shaping (possibly up to Middle Pleistocene). Similarly, also the adjacent fault systems (UAFS, MAFS and BSPF – see also section 2) tend to diminish their throw towards the area of the PSDFS tips (figure 7). The bell-shaped curve of figure 7 is also evidence of the fact that, although some internal complexity exists, at the basin scale the PSDFS is evidence of a single slipping fault.

The length of the PSDFS and the location of its boundaries, as resulting from this approach, are represented in figure 11a, where the bell-shaped profile (white solid line) is shown with the topography and the fault splay traces.

Following this reasoning, the resulting overall length of the PSDFS approximates 19 km.

Our findings are in agreement with the results of Calderoni et al. (2012), which used observations of fault-zone trapped waves (FZTWs) to investigate the continuity of the L'Aquila mainshock causative fault at depth. The results of their study confirmed that the PSDFS could be considered a ~20 km-long continuous fault system.

These results, when compared with the 3 km-long coseismic centimetric ruptures observed in 2009 (figure 11a) and with the evidence for paleoearthquakes more energetic than the April 6, 2009 event (Cinti et al., 2011), suggest that the 19 km-long geomorphic expression of the PSDFS cannot have been built up by only repeated 2009-type earthquakes but by both surface ruptures of the whole 19 km-long structure (master rupture generating the contemporaneous rupture of the northwestern and southeastern fault splays - P3, P2 and S6 – figure 10) and smaller sections ruptures. The normalized plot of figure 11b (data with polynomial interpolation of degree 3) compares the 2009 earthquake coseismic-slip distribution at the surface versus the PSDFS cumulative throw distribution, and shows clearly that the sole contribution of 2009-type earthquakes cannot explain the geomorphic expression of the whole system, thus suggesting a variable-slip behavior (Schwartz & Coppersmith, 1984).

According to the empirical relationships between magnitude and surface rupture length (Wells and Coppersmith, 1994), it appears clearly that the master ruptures are capable to produce more energetic earthquakes with respect to the 2009 event, with M up to 6.6, in agreement with the magnitude of several historical earthquakes occurred in the region (the 1349, 1703, and 1915 events were characterized by $M \geq 6.5$ and $I > 10$ MCS).

7 Conclusions

A detailed morphotectonic analysis allowed us to image the long-term morphological expression of the PSDFS and highlighted its geometrical arrangement (length, number of fault splays and boundaries) at the surface. We also defined a first-order hierarchy among the fault splays. This brought at a better understanding of the PSDFS Quaternary deformational history and of its seismic potential, thus contributing to the seismic hazard assessment in the area struck by the 2009 L'Aquila earthquake.

At a basin-wide scale, we highlighted the existence of a complex structural setting of the PSDFS at the surface, characterized by the presence of several parallel fault splays, frequently arranged in a quasi-fractal sequence of horst and graben of variable size. The PSDFS comprises two main sectors: (1) the Paganica sector to the NW, characterized by a narrow deformation zone and a relatively small Quaternary basin affected by few fault splays and (2) the San Demetrio sector to the SE, with a set of parallel, km-spaced fault splays that exhume and dissect a wider Quaternary basin. Notwithstanding this internal complexity, on the basis of the displacement distribution, 1) we defined that the PSDFS behave as a single individual normal fault, 2) we set the fault boundaries that can be considered stationary at least for the last morphogenic phase (up to Middle Pleistocene) and 3) we defined a ~19 km-long structure.

On basis of the empirical relations proposed by Wells and Coppersmith (1994) for normal faults, this surface fault length allows allow for up to M 6.6 earthquakes.

That earthquakes larger than the 2009 one may be produced by the 2009-earthquake fault system is also suggested by morphotectonic considerations. In fact, 2009-like coseismic ruptures only cannot be responsible for the built up of the present expression of the PSDFS, characterized by several kms-long and tens to hundreds m-high cumulative fault scarps.

Most of the deformation along the PSDFS is accommodated by the two easternmost basin-bounding fault splays (P4 and S10) affecting mainly the bedrock. Among the fault splays affecting mainly the Quaternary deposits (last ~2Ma), fault splays P3, P2 and S6 play a major role. Interestingly, they appear aligned for a total length of ~15 km and likely represent the presently most active trace of the system. The recognition of this fault hierarchy is particularly relevant for the assessment of surface faulting hazard and for the definition of correct set-back values. This topic is especially relevant because it often determines a substantial risk for urban areas and/or important infrastructures and facilities (roads, railways, pipelines, etc.). This was actually the case of the 2009 L'Aquila earthquake, where even though ruptures where centimetric, buildings and lifelines located in coincidence (on top/near) of the observed coseismic surface ruptures suffered significant damage (e.g. the Tempera aqueduct pipe broke because crossed by coseismic ruptures).

From a methodological point of view, this work took advantage on the availability of high-resolution (1 m) topographic data derived from an airborne LiDAR survey. The L'Aquila experience is the first in Italy and one of the very few in Europe that shows a tectonic application of airborne LiDAR technology, that, as already proven in other worldwide experiences, has been found to have a very high potential in detecting even subtle tectonic signatures (Haugerud et al., 2003; Sherrod et al., 2004; Cunningham et

al., 2006; Kondo et al., 2008; Arrowsmith and Zielke, 2009; Begg and Mouslopoulou, 2010; Hunter et al., 2011; Lin et al., 2013). Under this light, fault mapping integrating LiDAR to the other traditional approaches, is certainly an innovative and effective tool that represents an essential input for seismic hazard assessment and surface faulting hazard evaluation, especially in areas of high tectonic complexity (e.g. Vittori et al., 1997; Eurocode 8, 2003; Boncio et al., 2012; Civico et al., 2014).

Acknowledgement
We wish to thank Francesca Romana Cinti, Carlo Alberto Brunori and Fabio Villani for helpful discussions and advice. The airborne LiDAR survey performed by the Civil Protection of Friuli Venezia Giulia (Italy) was kindly released by Italian Civil Protection Department.
The work has been financially supported by the project "FIRB Abruzzo - High-resolution analyses for assessing the seismic hazard and risk of the areas affected by the 6 April 2009 earthquake".
Tectonophysics Editor Hans Thybo and Reviewer Vasiliki Mouslopoulou are acknowledged for providing constructive comments.
The views and conclusions contained in this study are those of the authors and are purely scientific, and they should not be interpreted as necessarily representing official policies, either expressed or implied, of the Istituto Nazionale di Geofisica e Vulcanologia (INGV).

References

- Amos, C. B., K. I. Kelson, D. H. Rood, D. T. Simpson and R. S. Rose, 2010. Late Quaternary slip rate on the Kern Canyon Fault at Soda Spring, Tulare County, California. Lithosphere, 2(6):411-417.
- Arrowsmith, J. R., O. Zielke, 2009. Tectonic geomorphology of the San Andreas Fault zone from high resolution topography: An example from the Cholame segment. Geomorphology, doi:10.1016/j.geomorph.2009.01.002.
- Atzori, S., I. Hunstad, M. Chini, S. Salvi, C. Tolomei, C. Bignami, S. Stramondo, E. Trasatti, and A. Antonioli, 2009. Finite fault inversion of DInSAR coseismic displacement of the 2009 L'Aquila earthquake (central Italy). Geophys. Res. Lett., 36, L15305. doi:10.1029/ 2009GL039293.
- Bagnaia, R., A. D'Epifanio, and S. Sylos Labini, 1992. Aquila and sub-aequan basins: an example of Quaternary evolution in central Apennines, Italy. Quat. Nova, II, 187–209.
- Begg, J. G. and V. Mouslopoulou, 2010. Analysis of late Holocene faulting within an active rift using lidar, Taupo Rift, New Zealand. Journal of Volcanology and Geothermal Research, 190, 152–167, doi:10.1016/j.jvolgeores.2009.06.001.
- Bertini, T. & Bosi, C. (1993), La tettonica quaternaria della conca di Fossa (L'Aquila). Il Quaternario, 6, 293-314.
- Blumetti, A,M., Guerrieri, L., and Vittori, E., 2013. The primary role of the Paganica-San Demetrio fault system in the seismic landscape of the Middle Aterno Valley basin (Central Apennines). Quaternary International, Volume 288, 4 March 2013, Pages 183-194, ISSN 1040-6182, http://dx.doi.org/10.1016/j.quaint.2012.04.040.
- Boncio, P., G. Lavecchia and B. Pace, 2004. Defining a model of 3D seismogenic sources for Seismic Hazard Assessment applications: the case of central Apennines (Italy). J. Seismol., 8(3), 407–425.
- Boncio, P., A. Pizzi, F. Brozzetti, G. Pomposo, G. Lavecchia, D. Di Naccio and F. Ferrarini, 2010. Coseismic ground deformation of the 6 April 2009 L'Aquila earthquake (central Italy, Mw6.3). Geophys. Res. Lett., 37, L06308, doi:10.1029/2010GL042807.
- Boncio, P., Galli, P., Naso, G. & Pizzi, A., 2012. Zoning Surface Rupture Hazard along Normal Faults: Insight from the 2009 Mw 6.3 L'Aquila, Central Italy, Earthquake and Other Global Earthquakes. Bulletin of the Seismological Society of America, Vol. 102, No. 3, June 2012, doi: 10.1785/0120100301.

- Bonini, L., Di Bucci, D., Toscani, G., Seno, S., and Valensise, G., 2013. A reversed hierarchy of active normal faults: the 6 April 2009, Mw 6.3, L'Aquila earthquake (Italy). Solid Earth Discuss., 5, 117-134, doi:10.5194/sed-5-117-2013, 2013
- Bosi, C., Bertini, T., 1970. Geologia della media valle dell'Aterno. Memorie Società Geologica Italiana 9, 719-777.
- Brunori, C.A., Civico, R., Cinti, F.R., Ventura, G., 2012. Characterization of active fault scarps from LiDAR data: a case study from Central Apennines (Italy). International Journal of Geographical Information Science, iFirst, 2012, 1-12, doi:10.1080/13658816.2012.684385.
- Caputo, R., Chatzipetros, A., Pavlides, S., Sboras, S., 2013. The Greek Database of Seismogenic Sources (GreDaSS): state-of-the-art for northern Greece. Annals Of Geophysics, 55, 5, 2012; doi: 10.4401/ag-5168.
- Cartwright, J.A., Trudgill, B.D., Mansfield, C.S., 1995. Fault growth by segment linkage: an explanation for scatter in maximum displacement and trace length data from the Canyonlands Grabens of SE Utah. Journal of Structural Geology, Volume 17, Issue 9, September 1995, Pages 1319-1326, ISSN 0191-8141, 10.1016/0191-8141(95)00033-A.
- Cavinato, G.P., De Celles P.G., 1999. Extensional basins in the tectonically bimodal central Apennines fold-thrust belt, Italy: response to corner flow above a subducting slab in retrograde motion. Volume 27, Issue 10, October 1999, Pages 955-958.
- Chiarabba, C., Jovane, L. and R. Di Stefano, 2005. A new view of Italian seismicity using 20 years of instrumental recordings. Tectonophysics, 395, 251–268, doi:10.1016/j.tecto.2004.09.013.
- Chiaraluce, L., L. Valoroso, D. Piccinini, R. Di Stefano, and P. De Gori, 2011. The anatomy of the 2009 L'Aquila normal fault system (central Italy) imaged by high resolution foreshock and aftershock locations. J. Geophys. Res., 116, B12311, doi:10.1029/2011JB008352.
- Chiaraluce, L., 2012. Unraveling the complexity of Apenninic extensional fault systems: A review of the 2009 L'Aquila earthquake (Central Apennines, Italy). Journal of Structural Geology, Volume 42, September 2012, Pages 2-18, http://dx.doi.org/10.1016/j.jsg.2012.06.007.
- Cinti, F.R., Pantosti, D., De Martini, P.M. Pucci, S., Civico, R., Pierdominici, S., Cucci, L., Brunori, C.A., Pinzi, S. and Patera, A., 2011. Evidence for surface faulting events along the Paganica fault prior to The 6 April 2009 L'Aquila Earthquake Central Italy. J. Geophys. Res, 116, B07308, doi:10.1029/2010jb007988.
- Civico, R., 2012. Integrating new and traditional approaches for the estimate of slip-rates of active faults: examples from the Mw 6.3, 2009 L'Aquila earthquake area, Central Italy. PhD thesis, Alma Mater Studiorum - Università di Bologna, http://www.earth-prints.org/handle/2122/8478.
- Civico, R., Pantosti, D., Pucci, S., De Martini, P.M., 2014. The contribution of airborne LiDAR data to the assessment of surface faulting hazard for lifelines crossing active faults: an example from the Central Apennines, Italy. Engineering Geology for Society and Territory, Volume 5, Chapter 193, DOI: DOI: 10.1007/978-3-319-09048-1_193, G. Lollino et al. (eds.), Springer International Publishing Switzerland.
- Contreras, J. Anders, M.H. and Scholz, C.H., 2000. Growth of a normal fault system: Observations from the Lake Malawi basin of the east African rift. Journal of Structural Geology 22: 159–168, ISSN 0191-8141, 10.1016/S0191-8141(99)00157-1.
- Cowie, P. A., and C. H. Scholz, 1992. Growth of faults by accumulation of seismic slip. J. Geophys. Res., 97(B7), 11085–11095, doi:10.1029/92JB00586.
- CPTI Working Group, 2004. Catalogo Parametrico dei Terremoti Italiani, versione 2004 (CPTI04), INGV, Bologna. Available at: http://emidius.mi.ingv.it/CPTI04/.
- Cunningham, D., S. Grebby, K. Tansey, A. Gosar and V. Kastelic, 2006. Application of airborne LiDAR to mapping seismogenic faults in forested mountainous terrain, southeastern Alps, Slovenia. Geophys. Res. Lett., 33, L20308, doi:10.1029/2006GL027014.
- D'Agostino, N., Speranza, F., Funiciello, R., 1997. Le Brecce Mortadella dell'Appennino Centrale: primi risultati di stratigrafia magnetica. Il Quaternario 10, 385-388.
- D'Agostino, N., Mantenuto, S., D'Anastasio, E., Giuliani, R., Mattome, M., Calcaterra, S., Gambino, P., Bonci, L., 2011. Evidence for localized active extension in the central Apennines (Italy) from global positioning system observations. Geology, 39,4, 291-294. 10.1130/G31796.1. http://hdl.handle.net/2122/7049.

- Dawers, N.H., Anders, M.H., and Scholz, C.H., 1993. Growth of normal faults – Displacement-length scaling. Geology 21: 1107–1110, doi:10.1130/0091-7613(1993)021<1107:GONFDL>2.3.CO;2.
- DeLong, S. B., G. E. Hilley, M. J. Rymer and C. Prentice., 2010. Fault zone structure from topography: Signatures of en echelon fault slip at Mustang Ridge on the San Andreas Fault, Monterey County, California. Tectonics, 29, TC5003, doi:10.1029/2010TC002673.
- Dramis, F., Blumetti, A.M., 2005. Some considerations concerning seismic geomorphology and paleoseismology. Tectonophysics, 408, 1-4, 177-191, doi:10.1016/j.tecto.2005.05.032.
- Emergeo Working Group, 2010. Evidence for surface rupture associated with the Mw 6.3 L'Aquila earthquake sequence of April 2009 (central Italy). Terra Nova, 22, 1, 43-51, doi: 10.1111/j.1365-3121.2009.00915.x.
- EUROCODE 8, 2003. Design of structures for earthquake resistance: Foundations, retaining structures and geotechnical aspects. European Committee for Standardization (CEN), Brussels, http://www.cen.eu/cenorm/homepage.htm.
- Falcucci, E., S. Gori, E. Peronace, G. Fubelli, M. Moro, M. Saroli, B. Giaccio, P. Messina, G. Naso, G. Scardia, A. Sposato, M. Voltaggio, P. Galli and F. Galadini, 2009. The Paganica Fault and surface coseismic ruptures caused by the 6 April 2009 earthquake (L'Aquila, central Italy). Seism. Res. Lett, 80, 6, 940-950.
- Frankel, K. L., J. F. Dolan, R. C. Finkel, L. A. Owen and J. S. Hoeft, 2007. Spatial variations in slip rate along the Death Valley-Fish Lake Valley fault system determined from LiDAR topographic data and cosmogenic 10Be geochronology. Geophys. Res. Lett., 34, L18303, doi:10.1029/2007GL030549.
- Galadini, F., Messina, P., Giaccio, B., Sposato, A., 2003. Early uplift history of the Abruzzi Apennines (central Italy): available geomorphological constraints. Quaternary International, Volumes 101–102, 2003, Pages 125-135, ISSN 1040-6182, http://dx.doi.org/10.1016/S1040-6182(02)00095-2.
- Galadini F., Galli P., 2000. Active tectonics in the central Apennines (Italy) Input data for seismic hazard assessment. Nat Hazards 22, 225-270.
- Galli, P., F. Galadini, and D. Pantosti, 2008. Twenty years of paleoseismology in Italy. Earth Sci. Rev., 88, 89–117.
- Galli, P., Giaccio, B, Messina, P., 2010. The 2009 central Italy earthquake seen through 0.5 Myr-long tectonic history of the L'Aquila faults system. Quaternary Science Reviews, 29, 3768-3789, doi:10.1016/j.quascirev.2010.08.018.
- Galli, P., Giaccio, B., Messina, P., Peronace, E., Zuppi, G. Maria, 2011. Palaeoseismology of the L'Aquila faults (central Italy, 2009, Mw 6.3 earthquake): implications for active fault linkage. Geophysical Journal International, doi 10.1111/j.1365-246X.2011.05233.x.
- Gasperini, P., G. Vannucci, D. Tripone and E. Boschi, 2010. The location and sizing of historical earthquakes using the attenuation of macroseismic intensity with distance. Bull. Seism. Soc. Am., 100, 5A, 2035-2066, doi:10.1785/0120090330.
- Giaccio, B., Galli, P., Messina, P., Peronace, E., Scardia, G., Sottili, G., Sposato, A., Chiarini, E., Jicha, B., Silvestri, S., 2012. Fault and basin depocentre migration over the last 2 Ma in the L'Aquila 2009 earthquake region, central Italian Apennines. Quaternary Science Reviews, Volume 56, 21 November 2012, Pages 69-88, ISSN 0277-3791, 10.1016/j.quascirev.2012.08.016.
- Gori S., Falcucci E., Atzori S., Chini M., Moro M., Serpelloni, E., Fubelli G., Saroli M., Devoti R., Stramondo S., Galadini, F. & Salvi S., 2012. Constraining primary surface rupture length along the Paganica fault (L'Aquila earthquake) with geological and geodetic (DInSAR and GPS) evidence. Ital. J. Geosci. (Boll. Soc. Geol. It.), Vol. 131, No. 3 (2012), doi: 10.3301/IJG.2012.21.
- Haugerud, R. A., D. J. Harding, S. Y. Johnson, J. Harless, C. S. Weaver and B. L. Sherrod, 2003. High-resolution lidar topography of the Puget Lowland, Washington - A bonanza for earth science. GSA Today, v. 13, no. 6, p. 4–10.
- Herrmann, R.B., Malagnini, L. and Munafò, I., 2011. Regional Moment Tensors of the 2009 L'Aquila Earthquake Sequence. Bull. Seismol. Soc. Am., 101, 3, 975–993, doi: 10.1785/0120100184.
- Hilley, G. E., S. DeLong, C. Prentice, K. Blisniuk and J. R. Arrowsmith, 2010. Morphologic dating of fault scarps using airborne laser swath mapping (ALSM) data. Geophys. Res. Lett., 37, L04301, doi:10.1029/2009GL042044.

- Hunstad, I., G. Selvaggi, N. D, Agostino, P. England, P. Clarke, and M. Pierozzi, 2003. Geodetic strain in peninsular Italy between 1875 and 2001. Geophys. Res. Lett., 30, 1181, doi:10.1029/2002GL016447, 4.
- Hunter L.E., Howle, J.F., Rose, R.S. & Bawden, G.W., 2011. LiDAR-Assisted Identification of an Active Fault near Truckee, California. Bulletin of the Seismological Society of America, vol. 101 (3), p. 1162-1182.
- Improta, L., Villani, F., Bruno, P.P., Castiello, A., De Rosa, D., Varriale, F., Punzo, M., Brunori, C.A., Civico, R., Pierdominici, S., Berlusconi, A., Giacomuzzi, G., 2012. High-resolution controlled-source seismic tomography across the Middle Aterno basin in the epicentral area of the 2009, Mw 6.3, L'Aquila earthquake (central Apennines, Italy). Ital. J. Geosci. (Boll. Soc. Geol. It.), Vol. 131, No. 3 (2012), pp. 373-388, doi: 10.3301/IJG.2011.35.
- ISIDe Working Group (INGV, 2010). Italian Seismological Instrumental and parametric database: http://iside.rm.ingv.it .
- King, G. C. P., R. S. Stein, and J. B. Rundle, 1988. The Growth of Geological Structures by Repeated Earthquakes 1. Conceptual Framework. J. Geophys. Res., 93(B11), 13307–13318, doi:10.1029/JB093iB11p13307.
- Kondo, H., S. Toda, K. Okumura, K. Takada and T. Chiba, 2008. A fault scarp in an urban area identified by LiDAR survey: A Case study on the Itoigawa–Shizuoka Tectonic Line, central Japan. Geomorphology, Volume 101, Issue 4, 1, Pages 731-739, ISSN 0169-555X, 10.1016/j.geomorph.2008.02.012.
- Lin, Z., Kaneda, H., Mukoyama, S., Asada, N., Chiba, T., 2013. Detection of subtle tectonic–geomorphic features in densely forested mountains by very high-resolution airborne LiDAR survey. Geomorphology, Volume 182, 15 January 2013, Pages 104-115, ISSN 0169-555X, 10.1016/j.geomorph.2012.11.001.
- Malinverno, A., and W. B. F. Ryan, 1986. Extension in the Tyrrhenian Sea and shortening in the Apennines as result of arc migration driven by sinking of the lithosphere. Tectonics, 5(2), 227–245, doi:10.1029/TC005i002p00227.
- Manzocchi, T., Walsh, J.J., Nicol, A., 2006. Displacement accumulation from earthquakes on isolated normal faults. Journal of Structural Geology, Volume 28, Issue 9, September 2006, Pages 1685-1693, ISSN 0191-8141, 10.1016/j.jsg.2006.06.006.
- Montone, P., Mariucci, M. T. and Pierdominici, S., 2012. The Italian present-day stress map. Geophysical Journal International, 189: 705–716. doi: 10.1111/j.1365-246X.2012.05391.x
- Moro, M., S. Gori, E. Falcucci, M. Saroli, F. Galadini, S. Salvi, 2013. Historical earthquakes and variable kinematic behaviour of the 2009 L'Aquila seismic event (central Italy) causative fault, revealed by paleoseismological investigations. Tectonophysics, Volume 583, 11 January 2013, Pages 131-144, http://dx.doi.org/10.1016/j.tecto.2012.10.036.
- Mouslopoulou, V., Walsh, J.J., Nicol, A., 2009. Fault displacement rates on a range of timescales. Earth and Planetary Science Letters, Volume 278, Issues 3–4, 25 February 2009, Pages 186-197, ISSN 0012-821X, 10.1016/j.epsl.2008.11.031.
- Nicol, A.,Walsh, J.J.,Watterson, J., Underhill, J.R., 1997. Displacement rates of normal faults. Nature 390, 157-159 (13 November 1997); doi:10.1038/36548.
- Nicol, A., Walsh, J., Berryman, K., Nodder, S., 2005. Growth of a normal fault by the accumulation of slip over millions of years. Journal of Structural Geology, Volume 27, Issue 2, February 2005, Pages 327-342, ISSN 0191-8141, 10.1016/j.jsg.2004.09.002.
- Papanikolaou, I. D., M. Foumelis, I. Parcharidis, E. L. Lekkas, and I. G. Fountoulis, 2010. Deformation pattern of the 6 and 7 April 2009, MW=6.3 and MW=5.6 earthquakes in L'Aquila (Central Italy) revealed by ground and space based observations. Nat. Hazards Earth Syst. Sci., 10, 73-87, doi:10.5194/nhess-10-73-2010.
- Perea, H., Masana, E., and Santanach, P., 2006. A Pragmatic Approach to Seismic Parameters in a region with Low Seismicity: The Case of Eastern Iberia. Natural Hazards, December 2006, Volume 39, Issue 3, pp 451-477.
- Pondrelli, S., S. Salimbeni, A. Morelli, G. Ekström, M. Olivieri and E. Boschi, 2010. Seismic moment tensors of the April 2009, L'Aquila (Central Italy), earthquake sequence. Geophys. J. Int. doi:10.111/j.1365-246X.2009.04418.x.

- Pucci, S., F. Villani, R. Civico, D. Pantosti, P. Del Carlo, A. Smedile, P. M. De Martini, E. Pons-Branchu, A. Gueli, 2014. Quaternary geology of the Middle Aterno Valley, 2009 L'Aquila earthquake area (Abruzzi Apennines, Italy). Journal of Maps, 06/2014; DOI: 10.1080/17445647.2014.927128.
- Schwartz, D. P. and K. J. Coppersmith, 1984. Fault Behavior and Characteristic Earthquakes: Examples From the Wasatch and San Andreas Fault Zones. J. Geophys. Res., 89(B7), 5681–5698, doi:10.1029/JB089iB07p05681.
- Servizio Geologico d'Italia, 2006. Foglio 359 L'Aquila. Carta Geologica d'Italia alla scala 1:50.000. SELCA, Firenze.
- Sherrod, B.L., Brocher, T.M., Weaver, C.S., Bucknam, R.C., Blakely, R.J., Kelsey, H.M., Nelson, A.R. and Haugerud R., 2004. Holocene fault scarps near Tacoma, Washington, USA Geology, January, 2004, v. 32, p. 9-12, doi:10.1130/G19914.1 .
- Stein, R. S., G. C. P. King, and J. B. Rundle, 1988. The Growth of Geological Structures by Repeated Earthquakes 2. Field Examples of Continental Dip-Slip Faults. J. Geophys. Res., 93(B11), 13319–13331, doi:10.1029/JB093iB11p13319.
- Tertulliani, A., Rossi, A., Cucci, L., Vecchi, M., 2009. L'Aquila (Central Italy) earthquake: the predecessors of the April 6, 2009 event. Seismological Research Letters 80, 1008–1013. http://dx.doi.org/10.1785/gssrl.80.6.1008.
- Trasatti, E., C. Kyriakopoulos and M. Chini, 2011. Finite element inversion of DInSAR data from the Mw 6.3 L'Aquila earthquake, 2009 (Italy). Geophys. Res. Lett., 38, L08306, doi:10.1029/2011GL046714.
- Vannoli, P., Burrato, P., Fracassi, U., Valensise, G., 2012. A fresh look at the seismotectonics of the Abruzzi (Central Apennines) following the 6 April 2009 L'Aquila earthquake (Mw 6.3). Ital. J. Geosci. (Boll. Soc. Geol. It.), Vol. 131, No. 3 (2012), pp. 309-329, doi: 10.3301/IJG.2012.03.
- Vezzani, L. and F. Ghisetti, 1998. Carta Geologica dell'Abruzzo, Scala 1:100,000. S.EL.CA., Firenze.
- Wallace, R. E., 1977. Profiles and ages of young fault scarps, north-central Nevada. Geological Society of America Bulletin 88, 1267-1281.
- Walters, R. J., J. R. Elliott, N. D'Agostino, P. C. England, I. Hunstad, J. A. Jackson, B. Parsons, R. J. Phillips and G. Roberts, 2009. The 2009 L'Aquila earthquake (central Italy): A source mechanism and implications for seismic hazard. Geophys. Res. Lett., 36, L17312, doi:10.1029/2009GL039337.
- Wells, D.L. and K.J. Coppersmith, 1994. New empirical relationships among Magnitude, rupture length, rupture width, rupture area, and surface displacement. Bull. Seismol. Soc. Am., 84, 974-1002.
- Villani, F., Pucci, S., Civico, R., De Martini, P.M., Nicolosi, I., D'Ajello Caracciolo, F., Carluccio, R., Di Giulio, G., Vassallo, M., Smedile, A. and D. Pantosti, 2014. Imaging the structural style of an active normal fault through multi - disciplinary geophysical investigation: a case study from the Mw 6.1, 2009 L'Aquila earthquake region (central Italy). In press on Geophys. J. Int.
- Vittori, E., Maschio, L., Ferreli, L., Michetti., A.M., Serva, L., 1997. Carta e base di dati delle faglie capaci per l'Italia centro-meridionale: presentazione e stato di avanzamento del progetto ITHACA. Il Quaternario – Italian Journal of Quaternary Sciences, 10(2), 1997, 305-312.
- Vittori, E., Di Manna, P., Blumetti, A.M., Comerci, V., Guerrieri, L., Esposito, E., Michetti, A.M., Porfido, S., Piccardi, L., Roberts, G.P., Berlusconi, A., Livio, F., Sileo, G., Wilkinson, M., Mccaffrey, K.J.W., Phillips, R.J. & Cowie, P.A., 2011. Surface Faulting of the 6 April 2009 Mw 6.3 L'Aquila Earthquake in Central Italy. Bull. Seism. Soc. Am., 101 (4), 1507-1530. Doi:10.1785/0120100140.

Figures captions

Figure 1 *- The 2009 L'Aquila seismic sequence as recorded by the INGV Italian National Seismic Network (ISIDe Working Group (INGV, 2010), Italian Seismological Instrumental and parametric database: http://iside.rm.ingv.it) for the time period 6 April 2009 through 31 December 2009. The symbol size is proportional to the magnitude bin. Focal mechanism of the main shock and of the two largest aftershocks (Pondrelli et al., 2010), historical seismicity (M > 5.0; http://emidius.mi.ingv.it/CPTI04), and active faults are shown (UAFS: Upper Aterno Fault System; LMFS: Laga Mountain Fault System; CIFS: Campo Imperatore Fault System; LMFS: Laga Mountain Fault System; AF: Assergi Fault; PF: Paganica Fault; SDF:*

San Demetrio Fault; MAFS: Middle Aterno Fault System; MO: Monti D'Ocre Fault; CF: Campo Felice Fault; OPS: Ovindoli-Pezza Fault, modified after Geologic Map of Italy – Servizio Geologico d'Italia, 2006 and after Galli et al., 2008). The yellow box is the approximate projection to the surface of the ~16 km-long 2009 mainshock causative fault according to various investigators (see a review in Vannoli et al., 2012 and Chiaraluce, 2012). The inset shows the direction of extension across the central Apennines (black arrows) and the regional felt area for the 6 April mainshock (colored area).

***Figure 2** – Distribution of the coseismic surface ruptures in the eastern side of the Middle Aterno valley. Yellow triangles represent continuous coseismic surface ruptures; green triangles are discontinuous open fissures. The orange box is the approximate projection to the surface of the ~16 km-long 2009 mainshock causative fault according to various investigators (see a review in Vannoli et al., 2012 and Chiaraluce, 2012). Faults from literature: Pettino and Stabiata faults (UAFS), Middle Aterno Fault System (MAFS) and Barisciano - S.Pio Fault (BSPF) - modified after Geologic Map of Italy – Servizio Geologico d'Italia, 2006 and after Galli et al., 2008). a, b,c and d icons mark the approximate location of the photos in figure 3.*

***Figure 3 –** Examples of flat remnant surfaces used as piercing points to measure vertical throws (locations in figure 2). a) Paleomorphology related to a flat valley bed of an ancient drainage network (arrow showing approximate flow direction; b) Conglomeratic alluvial fan indicating an ancient southward feeding of the continental basin; c) depositional surfaces of alluvial Quaternary deposits; d) offset erosional (on bedrock) and depositional (alluvial Quaternary deposits) surfaces.*

***Figure 4** – Map of the 2009-earthquake fault system showing its geometrical arrangement at the surface and the extent and age of outcropping Pre-Quaternary, Plio-Pleistocene and Holocene deposits. The fault splays are named using different prefixes to differentiate between the Paganica and San Demetrio Ne' Vestini sectors (e.g. P1 stands for splay number 1 in the Paganica sector, S6 for splay number 6 in the San Demetrio Ne' Vestini sector). Black lines are the traces of the 29 topographic profiles across the fault system.*

***Figure 5** – a) Traces of the 36 topographic profile (black lines) across the 2009-earthquake fault system and adjacent fault systems (Pettino and Stabiata faults (UAFS), Middle Aterno Fault System (MAFS) and Barisciano - S.Pio Fault (BSPF). The traces of adjacent fault system are modified after Galli et al. (2008). b) Field picture showing one of the "Remnant top surfaces" (photo location marked with "b" icon in figure 5a).*

***Figure 6** - Examples of measurements made on topographic profiles. Vertical exaggeration associated to the topographic profiles is 3x. **a**) morphological throw, measured for each profile as the difference between the maximum elevation in the footwall of the fault system (in coincidence of the reference baseline - orange solid line in figure 5) and the elevation of the Middle Aterno basin floor at the hangingwall. **b**) measured morphological throws, represented by the vertical component of the separation (Vs) between an upper and a lower original reference erosional or depositional surface. When a reference surface is not clearly recognizable (both in the footwall or in the hangingwall), the morphological throw is expressed as the average of two possible Vs values (Vs1 and Vs2).*

***Figure 7** – Along-strike total morphological throw distribution of the main faults in the study area showing a decrease of throw values in coincidence with the overlap zones between different fault systems also coinciding with major drainage incisions.*

***Figure 8** – Along-strike plot of the morphological throws measured from the topographic profiles across the PSDFS. Morphological throws for each fault splay are shown in different colors and with different symbols to distinguish between throw values calculated from offset reference surfaces (i.e. piercing points) carved in bedrock (star) or in unconsolidated deposits (square) or a combination of the two (point).*

***Figure 9** - Along-strike plot of all the morphological throw values measured from the topographic profiles across the PSDFS. The red thick curve represents the sum of the relative contribution of each fault splay, while green and blue areas show the relative contribution of the fault splays (with exception of P4 and S10) affecting Quaternary sediments in the Paganica and San Demetrio sector, respectively.*

Figure 10 *- Map of the PSDFS showing the possible linkage of fault splays P3 and P2 (to the northwest) with S6 (to the southeast).*

Figure 11 *– **a**) overall length of the PSDFS as defined by the plot of the morphological throws. **b**) normalized plot (data with polynomial interpolation of degree 3) comparing the 2009 earthquake coseismic-slip distribution at the surface versus the PSDFS cumulative throw distribution.*

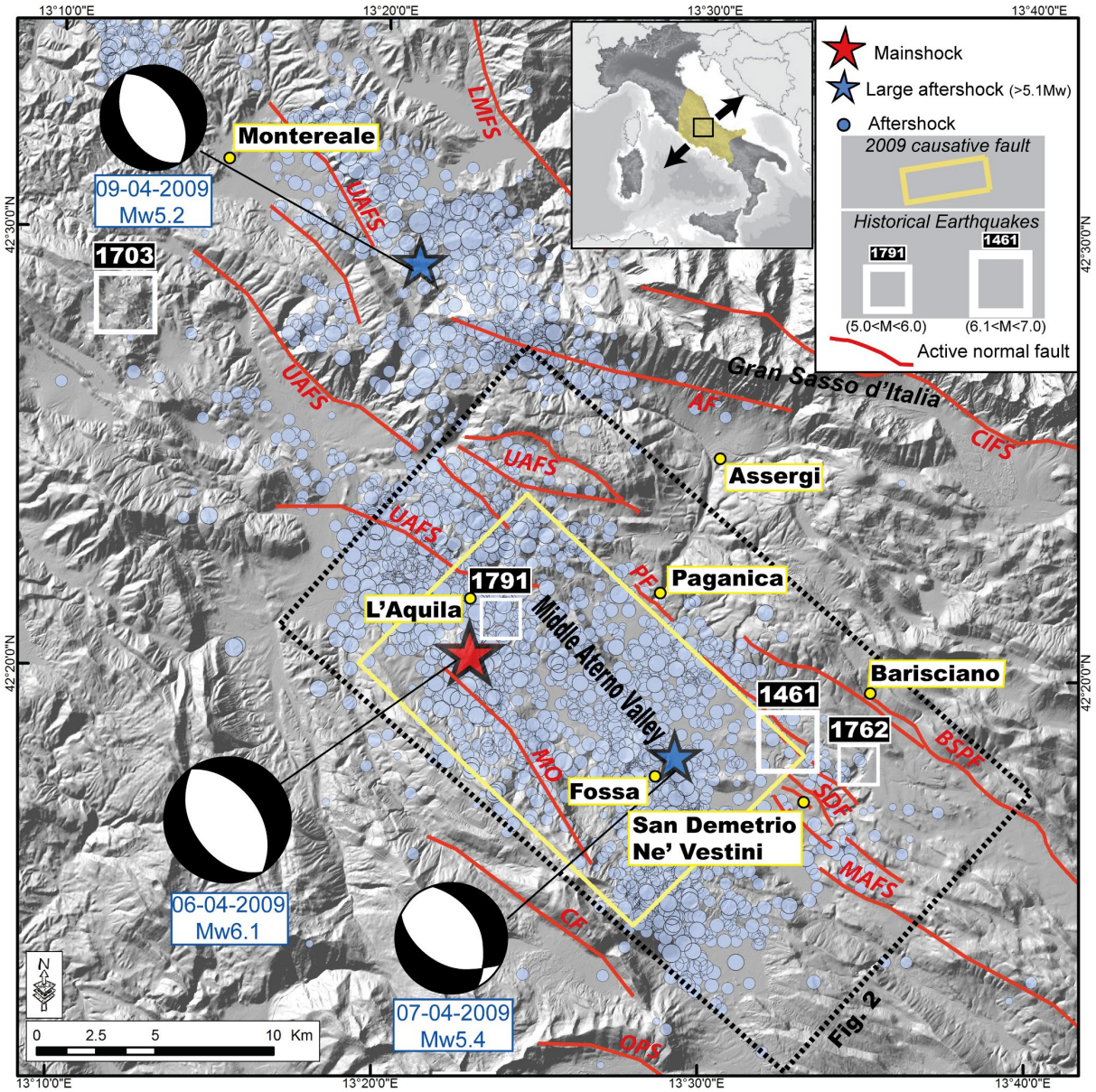

Figure 1

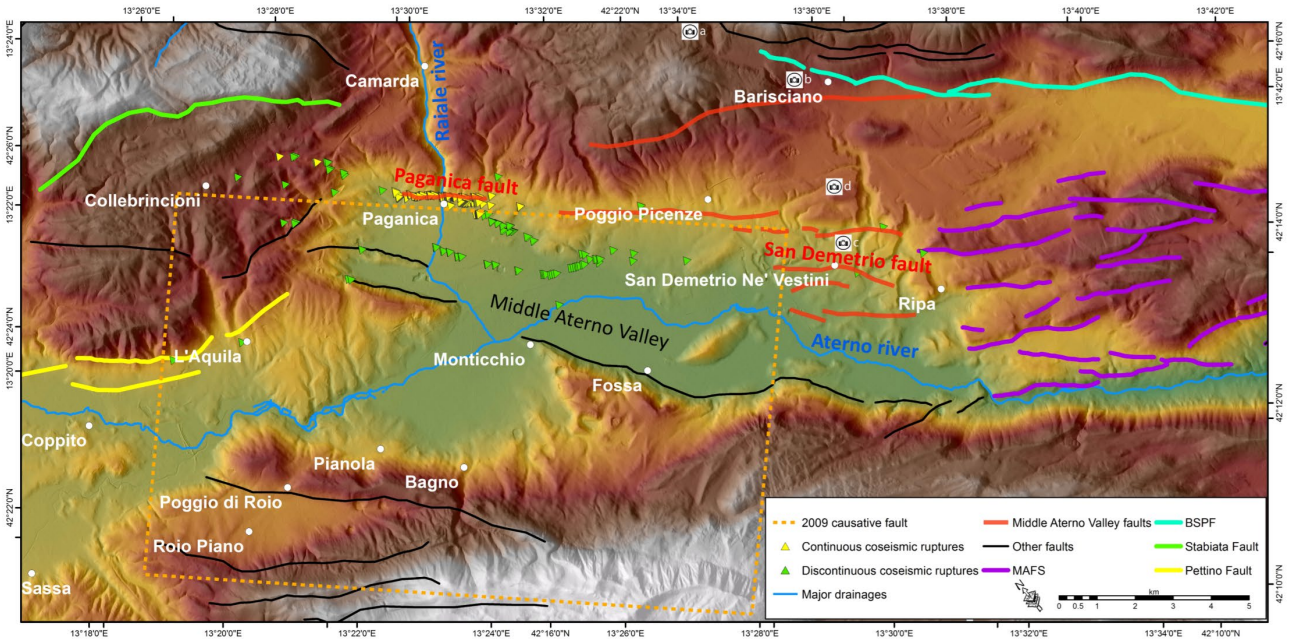

Figure 2

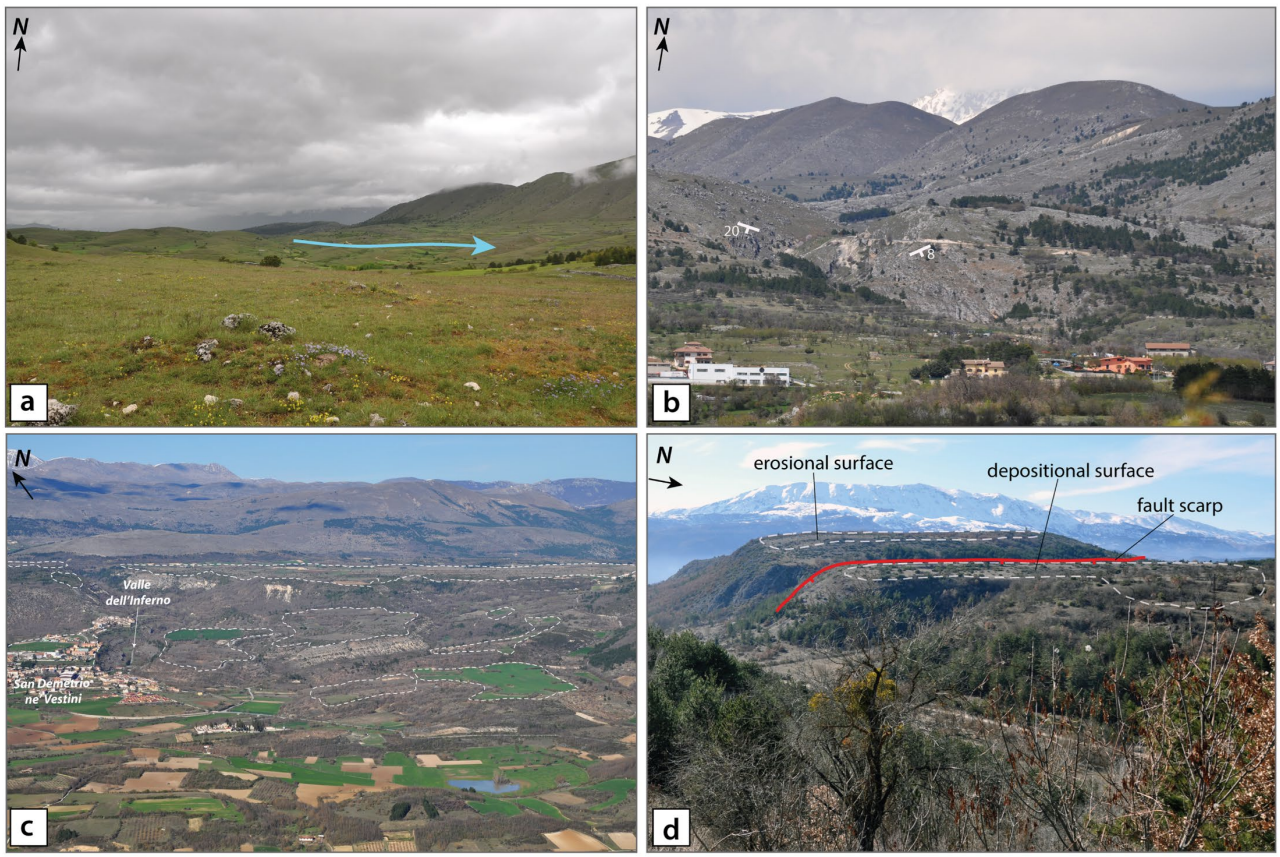

Figure 3

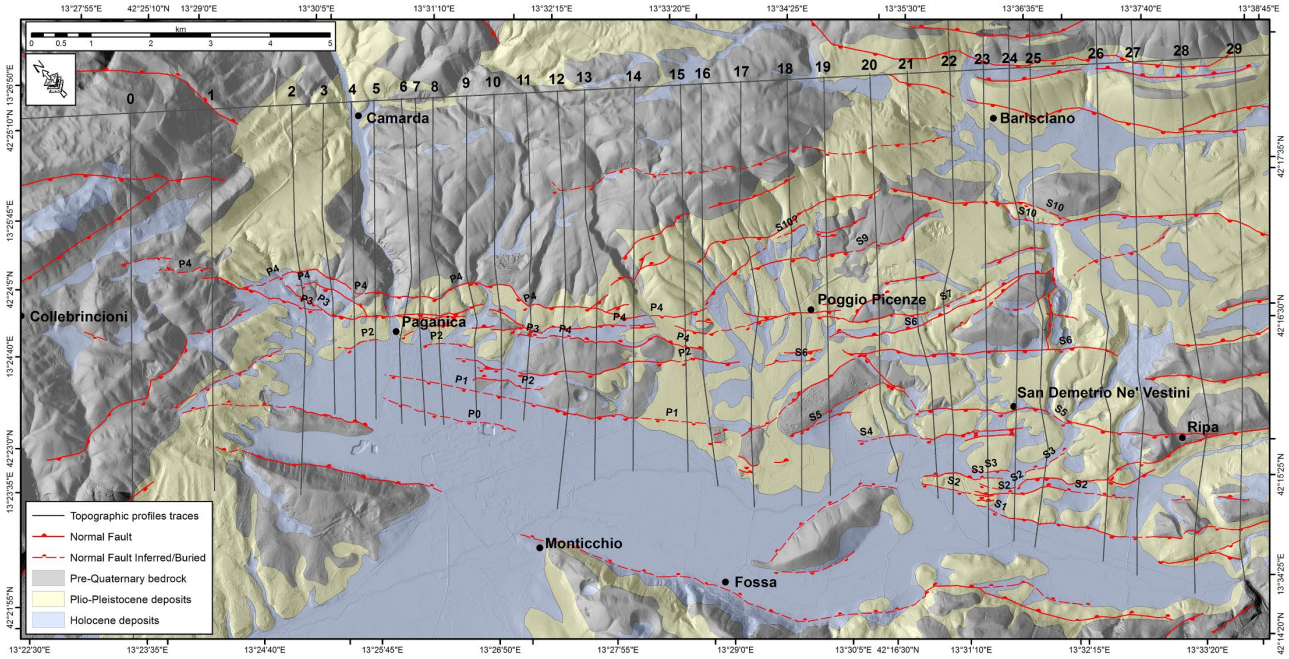

Figure 4

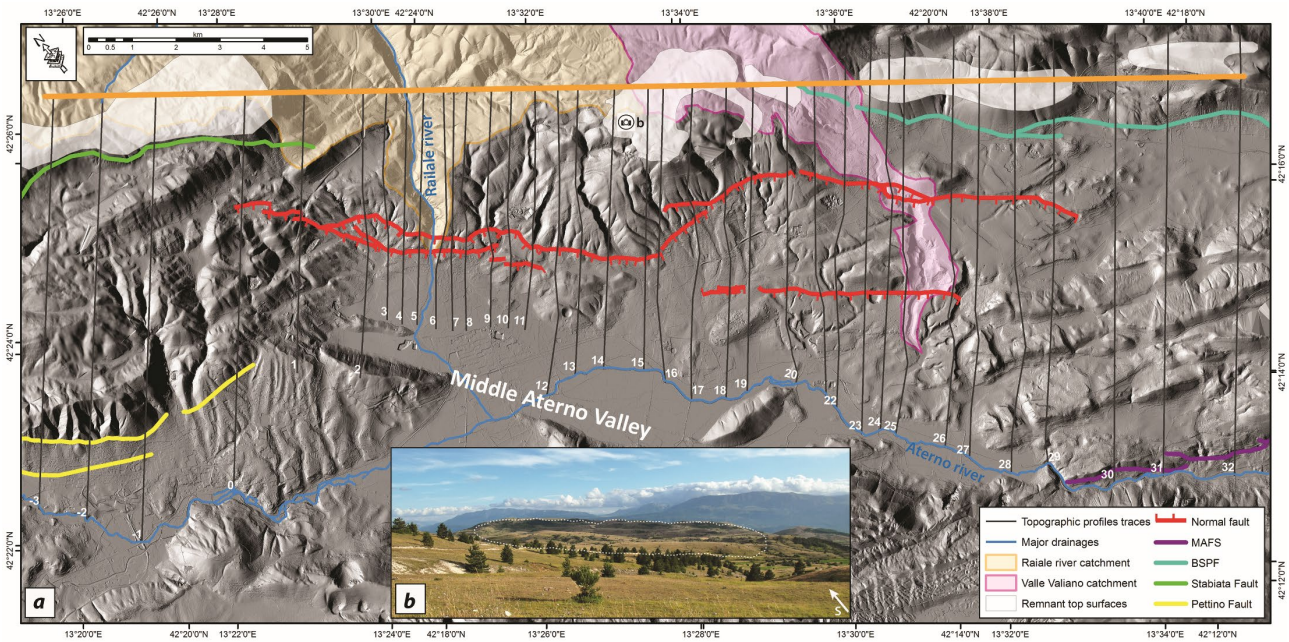

Figure 5

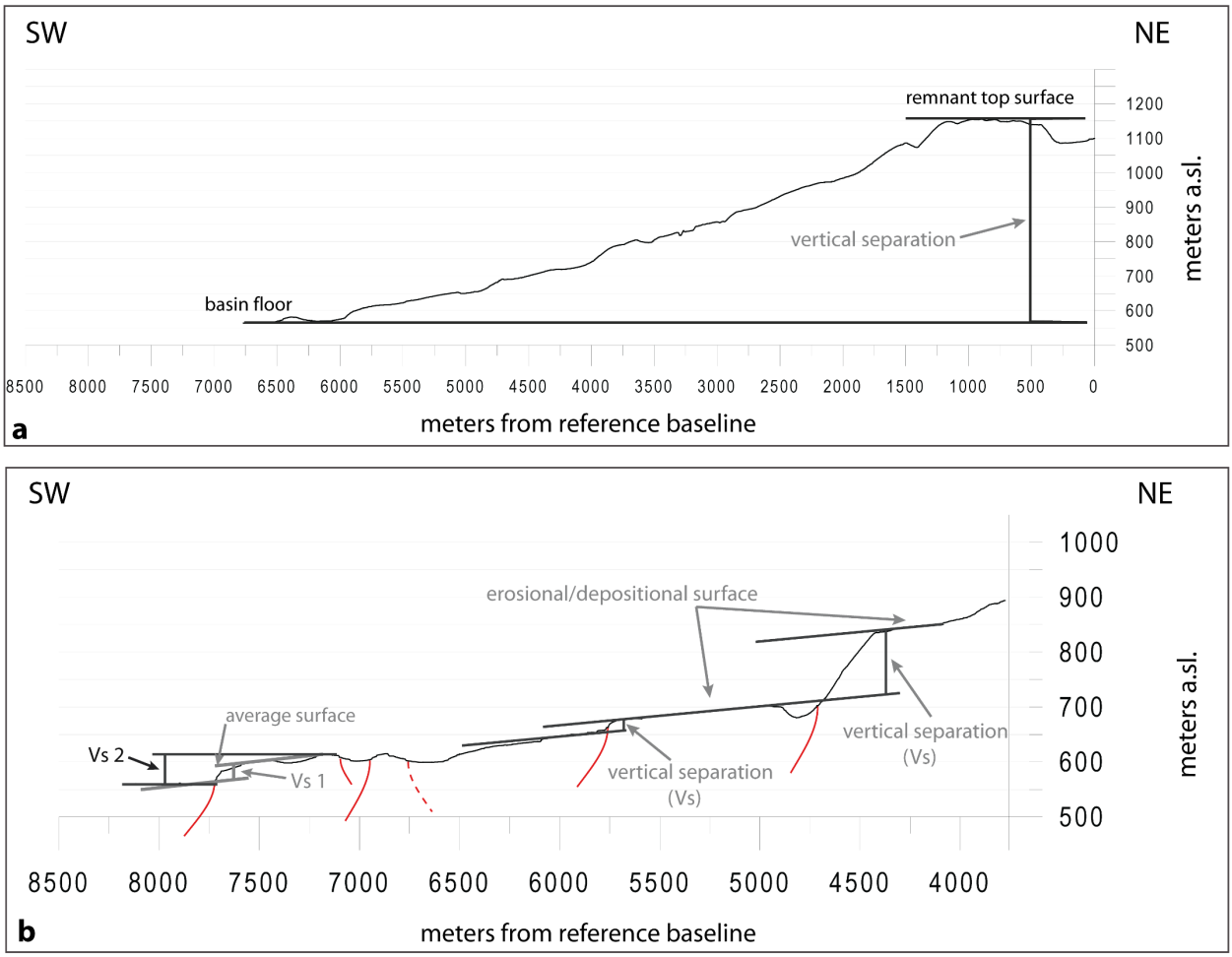
SW
NE
remnant top surface
vertical separation
basin floor
1200
1100
1000
900
800
700
600
500
meters a.sl.
8500 8000 7500 7000 6500 6000 5500 5000 4500 4000 3500 3000 2500 2000 1500 1000 500 0
a
meters from reference baseline
SW
NE
erosional/depositional surface
average surface
Vs 2
Vs 1
vertical separation (Vs)
vertical separation (Vs)
1000
900
800
700
600
500
meters a.sl.
8500 8000 7500 7000 6500 6000 5500 5000 4500 4000
b
meters from reference baseline

Figure 6

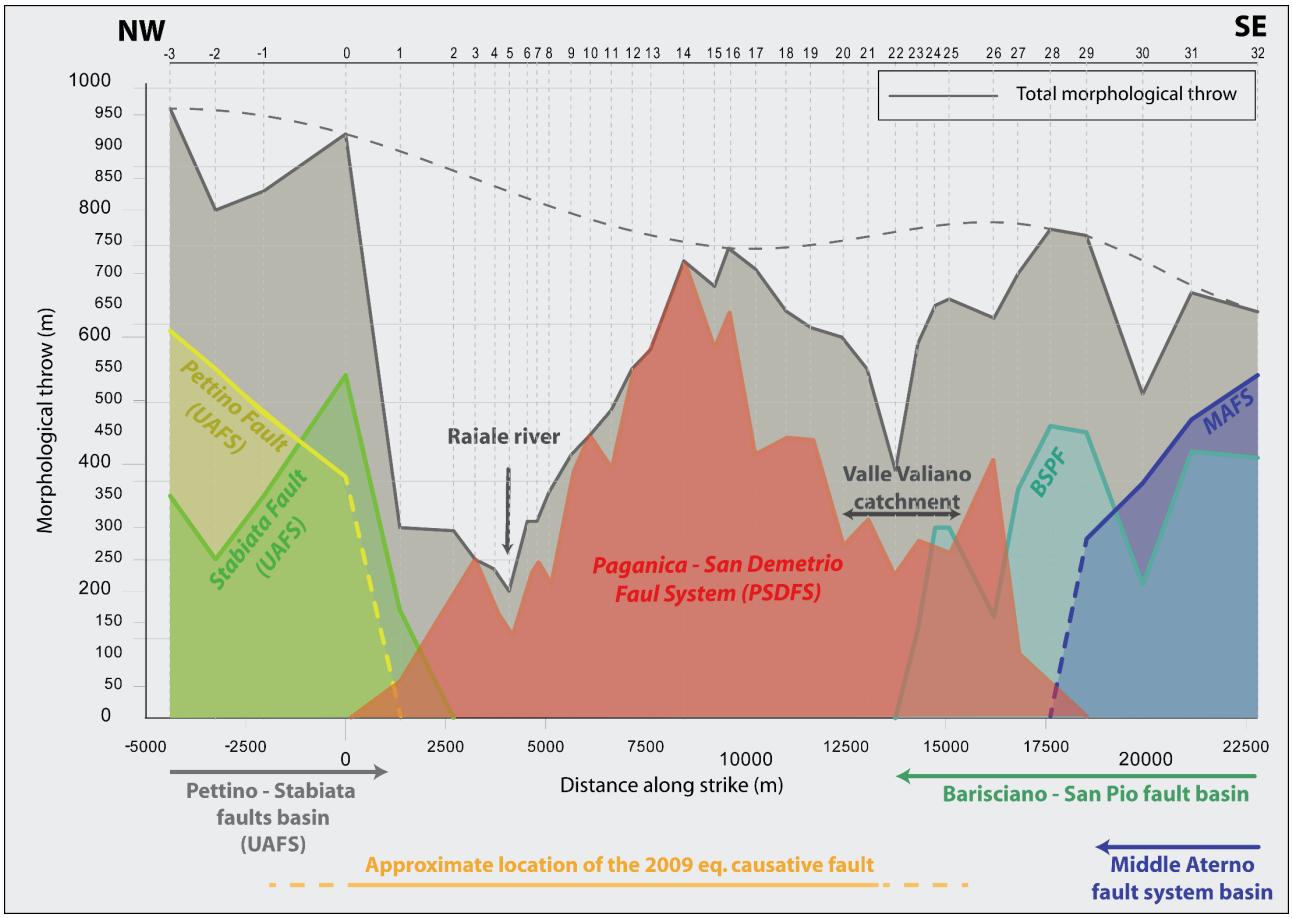

Figure 7

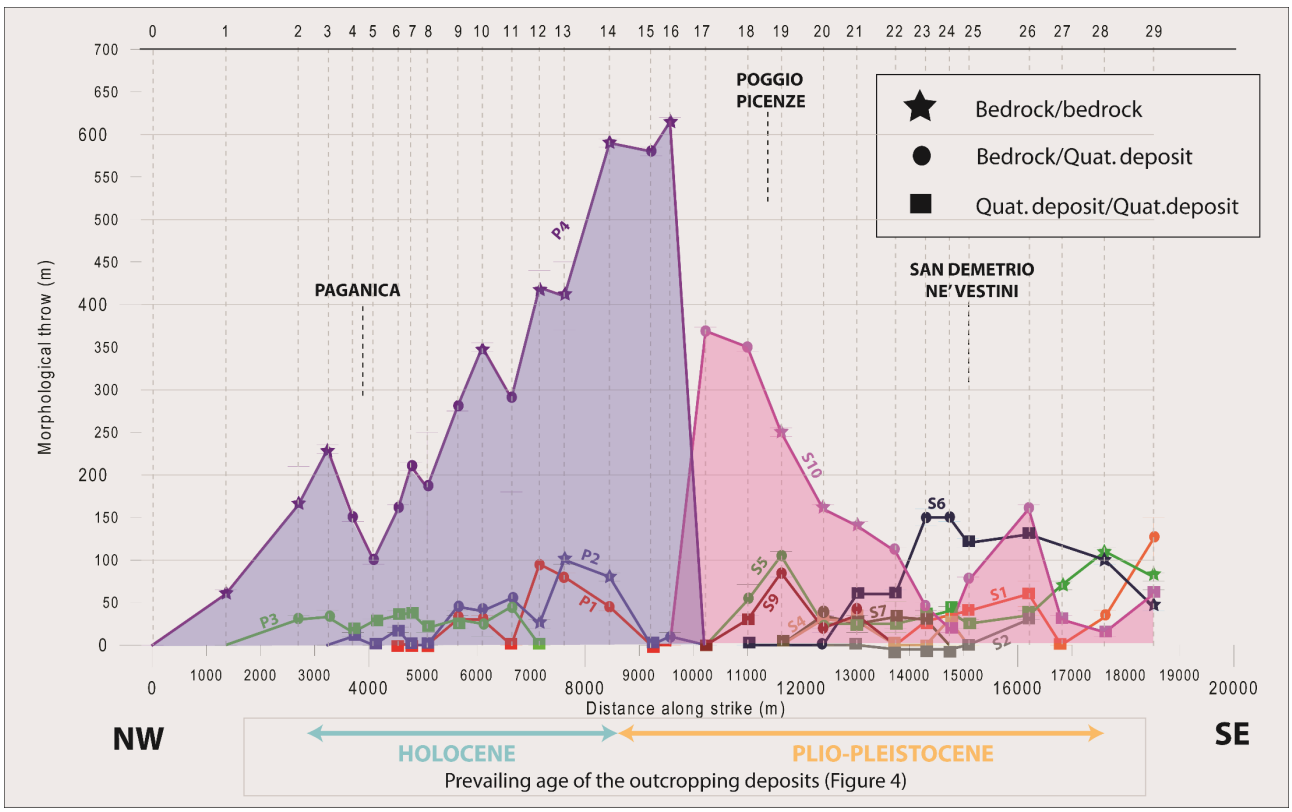

Figure 8

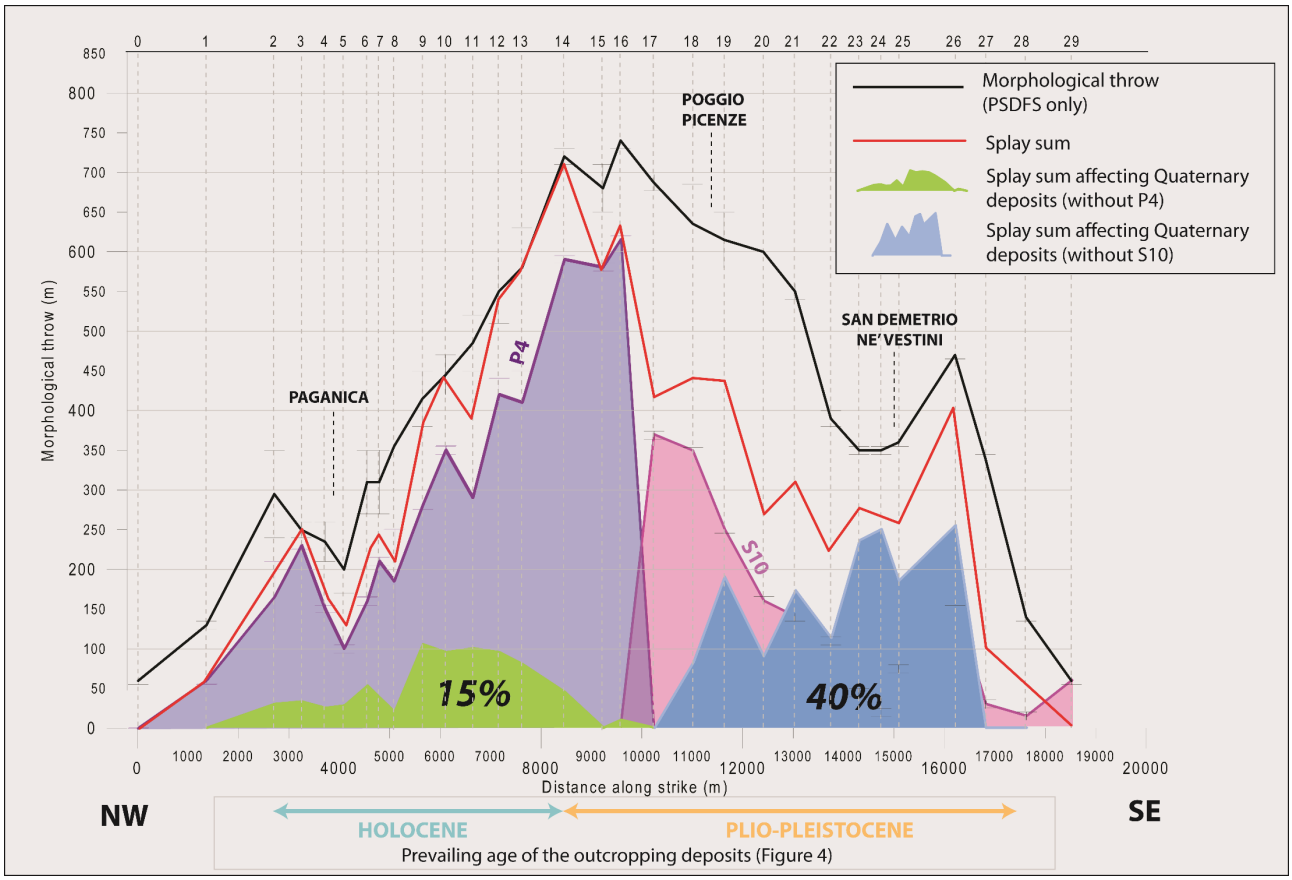
Morphological throw (PSDFS only)
Splay sum
Splay sum affecting Quaternary deposits (without P4)
Splay sum affecting Quaternary deposits (without S10)
POGGIO PICENZE
SAN DEMETRIO NE' VESTINI
PAGANICA
P4
S10
15%
40%
Morphological throw (m)
Distance along strike (m)
NW
SE
HOLOCENE
PLIO-PLEISTOCENE
Prevailing age of the outcropping deposits (Figure 4)

Figure 9

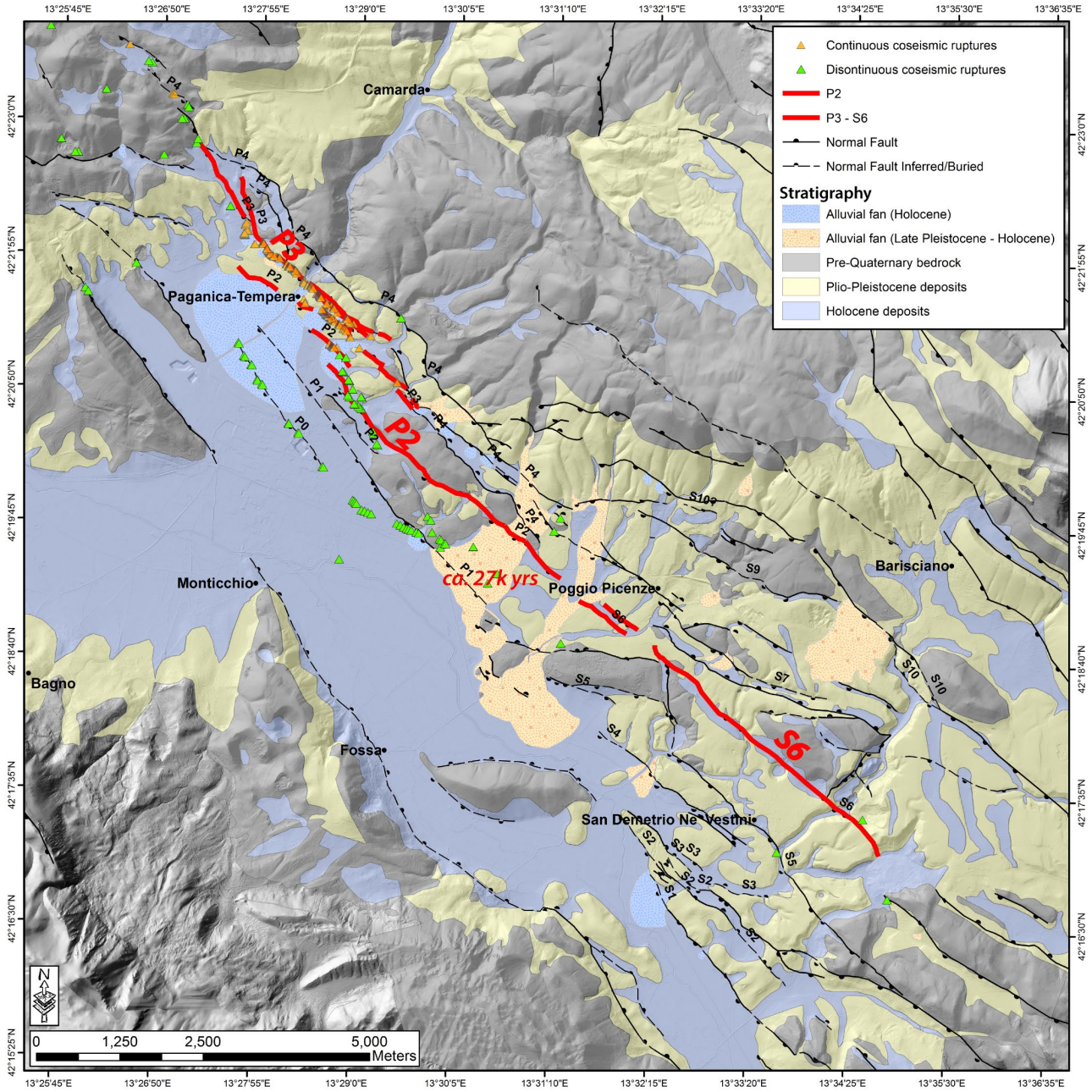
Continuous coseismic ruptures
Disontinuous coseismic ruptures
P2
P3 - S6
Normal Fault
Normal Fault Inferred/Buried
Stratigraphy
Alluvial fan (Holocene)
Alluvial fan (Late Pleistocene - Holocene)
Pre-Quaternary bedrock
Plio-Pleistocene deposits
Holocene deposits
Camarda
Paganica-Tempera
Monticchio
Bagno
Fossa
Poggio Picenze
Barisciano
San Demetrio Ne' Vestini
ca. 27k yrs
P3
P2
S6
0 1,250 2,500 5,000
Meters

Figure 10

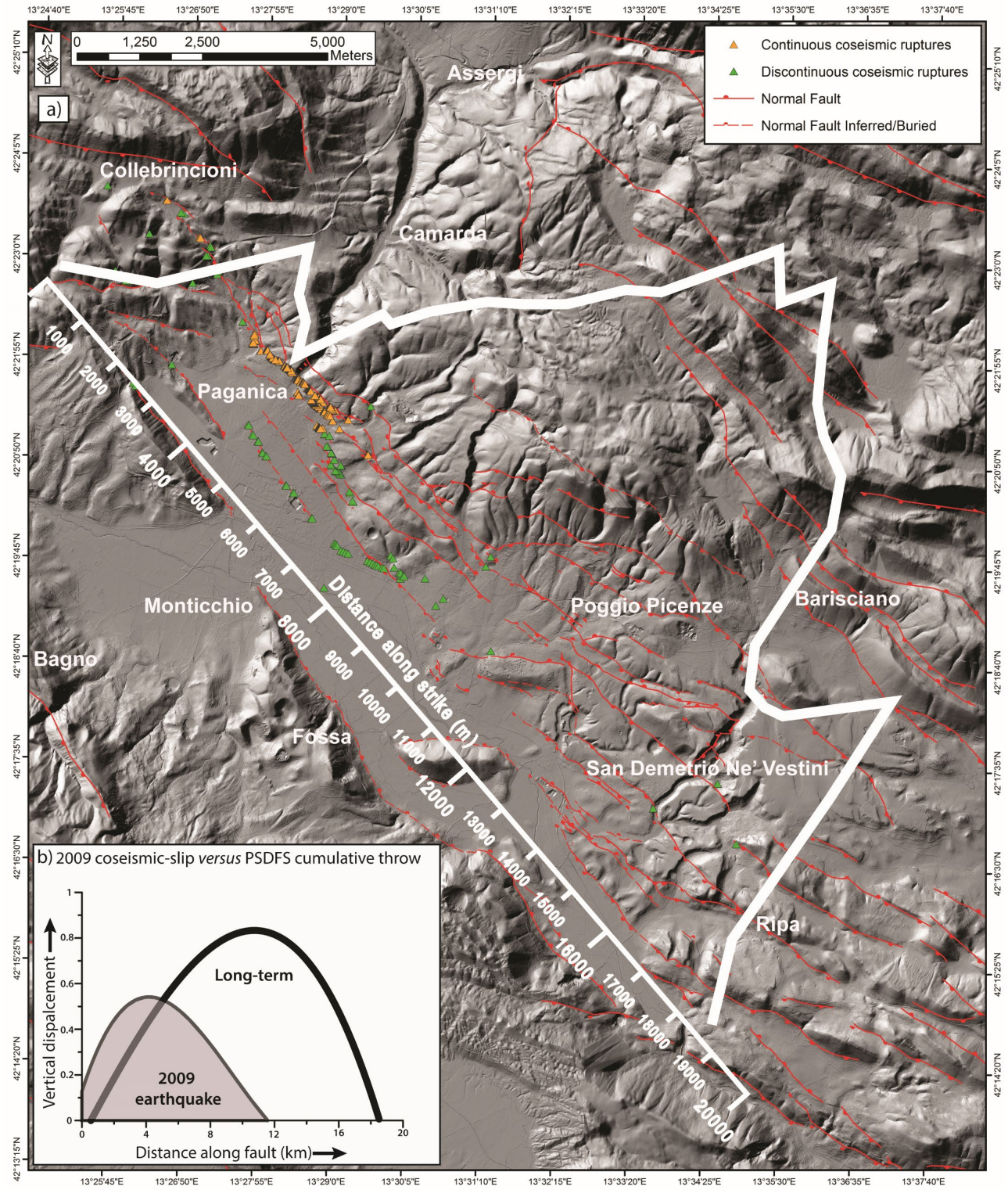
a)
0 1,250 2,500 5,000 Meters
Continuous coseismic ruptures
Discontinuous coseismic ruptures
Normal Fault
Normal Fault Inferred/Buried
Assergi
Collebrincioni
Camarda
Paganica
Monticchio
Bagno
Fossa
Poggio Picenze
Barisciano
San Demetrio Ne' Vestini
Ripa
Distance along strike (m)
1000
2000
3000
4000
6000
8000
7000
8000
9000
10000
11000
12000
13000
14000
15000
16000
17000
18000
19000
20000
b) 2009 coseismic-slip versus PSDFS cumulative throw
Vertical displacement
Long-term
2009 earthquake
Distance along fault (km)

Figure 11